J. Fluid Mech. (1999), *vol.* 380, *pp.* 39–57. Printed in the United Kingdom

On the propagation of oceanic mesoscale vortices

By TIMOUR RADKO AND MELVIN E. STERN

Oceanography Department, Florida State University, Tallahassee, FL 32306-4320, USA
e-mail: radko@ocean.fsu.edu; stern@ocean.fsu.edu

(Received 1 October 1997 and in revised form 20 August 1998)

An analytical theory is developed for a class of stable quasi-geostrophic vortices propagating either in the westward direction with supercritical velocities $(\bar{c} < -\beta \bar{R}_d^2)$ or eastward, where $\bar{R}_d$ is the radius of deformation and β is the gradient of the Coriolis parameter. The numerical spectral calculations, initiated by the theoretical solutions, indicate that the supercritical vortices move initially with the predicted velocity, but later slow down to the speed of the long planetary waves. The period of time during which an eddy is propagating with its initial velocity is analysed as a function of its strength and (initial) speed. The theoretical solution has a distinctive streamline signature ('alpha gyre'), which also appears in the final state of the numerical calculations, including those for an initially completely symmetric vortex placed on the β-plane.

1. Introduction

Among the most important characteristics of ocean eddies are their propagation velocities and their long lifetimes, which allow eddies to play an important role in large-scale mixing in the ocean. Agulhas eddies, for example, travel thousands of kilometres, transporting mass, vorticity, salinity and heat anomalies (Gordon & Haxby 1990). The observed westward drift of strong eddies is usually attributed to the meridional variation of the Coriolis parameter, the so-called β-effect (see Sutyrin & Flierl 1994). It has also been suggested (Sutyrin 1987) that the appearance of an azimuthal perturbation with mode number $m = 1$, caused by the β-effect, is responsible for the vortex translation (this mode is also referred to as a dipolar component or a vortex asymmetry). Estimates of the strength of such perturbations in the observed vortices were made by Mied, Lindemann & Bergin (1983) and Olson (1980). Recent measurements made with remote sensing imagery clearly confirmed the existence of a significant dipolar component in the observed synoptic eddies (Duncombe Rae *et al.* 1992; Hooker *et al.* 1995). However, the mechanism which allows an initially symmetric eddy (see McWilliams & Flierl 1979) to develop and maintain such north–south asymmetry for long periods of time is still poorly understood.

Some insight into the problem of vortex propagation was obtained by studies of exact permanent-form solutions with dipolar structure, referred to as modons (Stern 1975; Larichev & Reznik 1976). These were subsequently generalized by Flierl *et al.* (1980) to include a superimposed axisymmetric circulation (a 'rider'), but modons with riders are unstable (Swenson 1987) and this severely limits their ability to serve as models for observed synoptic eddies which are usually stable and nearly monopolar structures (Kamenkovich, Koshlyakov & Monin 1986).

In contrast to the exact (modon) solutions of the quasi-geostrophic equations, there are asymptotic theories appropriate to the geophysical situation in which the eddy translation speed is much smaller than the speed of the particles inside the eddy. For example, Stern (1987) found a barotropic solution for a piecewise uniform vorticity eddy bounded by two circular interfaces; a small separation between the centroids of the two interfaces produced a dipole moment, resulting in the propagation of the eddy. A generalization of this self-propagating f-plane vortex obtained by Stern & Radko (1998, hereinafter referred to as SR) showed that, for almost any compact circular vortex, an $m = 1$ disturbance resulting in the rectilinear motion of the eddy can be found. SR also developed a weakly nonlinear theory indicating that the eddy is able to traverse distances much larger than its radius without significant change of shape. Numerical experiments confirmed this conclusion, as well as the stability of some members of the family of self-propagating eddies. The specific dipolar component of such solutions will be referred to as an 'alpha-gyre', which is a term used in atmospheric science to describe a uniform (Gallilean) shift of a coordinate system (Willoughby 1992). On the other hand, the alpha-gyre in SR represents a dynamical effect, since the shift of the vorticity isopleths occurs only in the interior of the eddy and the exterior field is truly dipolar. These alpha-gyres are characterized by proportionality of the dipolar part of the streamfunction and the basic radial velocity in the interior. This important feature will also appear in the equivalent barotropic β-plane model considered herein.

Also important for understanding the dynamics of isolated eddies on the β-plane is a 'centroid theorem' (McWilliams & Flierl 1979) which states that the centroid of the interfacial height in a $1\frac{1}{2}$-layered ocean should propagate westward with exactly the Rossby wave signal velocity. Does this simple result imply that all geostrophic isolated eddies (non-modons) should propagate with the speed of the long Rossby waves? Such an assumption contradicts both observations (Chassignet, Olson & Boudra 1990) and intuition, which suggests that the propagation velocity should depend on various factors, such as the amplitude of the dipolar moment of the eddy. In the present paper we will attempt to clarify the issue by initially superimposing a certain dipolar component on a symmetric eddy, and numerically computing the evolution of the system in time. The results will suggest significant differences in the propagation of the centre of the eddy defined, for example, by the maximum of the potential vorticity, and the aforementioned height centroid.

This paper is organized as follows: in § 2 we introduce a theory for a quasi-geostrophic vortex which has a small $m = 1$ component (i.e. 'quasi-monopolar'), and which is assumed to propagate without change of shape either westward with velocity exceeding the speed of the long Rossby waves, or eastward; unlike a well-known exact solution (Flierl *et al.* 1980) our vortex will be stable. In § 3 we present numerical (spectral) calculations initiated by the theoretical solution. It will be shown that the westward propagating supercritical (i.e. moving faster than the speed of the long Rossby waves) eddies are able to preserve their velocity and dipolar moment for a significant time, after which they slow down to the speed of the long Rossby waves. In § 4 we demonstrate that an initially axisymmetric equivalent barotropic eddy, under the influence of a β-effect, develops the 'alpha-gyre' structure predicted by the analytic theory.

2. Equivalent-barotropic propagating vortices on the beta-plane

2.1. *Formulation*

Consider a mesoscale equivalent barotropic flow on the beta-plane that satisfies the non-dimensional equation for conservation of potential vorticity:

$$\frac{\partial}{\partial t}Q + J(\psi, Q) = 0, \tag{1}$$

where ψ is the streamfunction, and $Q = \Delta\psi - (1/R_d^2)\psi + y$ is the quasi-geostrophic potential vorticity; the horizontal coordinates here have been scaled by the eddy radius R, and the time coordinate by $\beta^{-1}R^{-1}$. In most of the following calculations we will consider the case where the non-dimensional Rossby radius of deformation $R_d = (g'H)^{1/2}/fR$ equals unity, but this can easily be extended to any value of $R_d = O(1)$.

Let us rewrite the equation of motion in a coordinate system moving in the x-direction with velocity c by applying the transformations

$$x_{old} = x_{new} + ct_{new}, \quad y_{old} = y_{new}, \quad t_{old} = t_{new}, \quad \psi_{old} = \psi_{new} - cy_{new}.$$

Then in terms of the new variables (subscripts are dropped for simplicity), equation (1) becomes

$$\frac{\partial}{\partial t}\left(\Delta\psi - \frac{1}{R_d^2}\psi\right) + J(\psi, \Delta\psi) + \hat{\beta}\frac{\partial\psi}{\partial x} = 0, \tag{2}$$

where

$$\hat{\beta} = 1 + c/R_d^2$$

is referred to as a modified beta (see, for example, Sutyrin & Flierl 1994). As in SR, an 'asymptotically valid' solution for a drifting system ($\partial/\partial t = 0$) will be sought, in which case (2) becomes

$$J(\psi, \Delta\psi + \hat{\beta}y) = 0. \tag{3}$$

We consider separately the region inside the unit circle streamline, and the exterior region with open streamlines surrounding the eddy. We assume that the total streamfunction

$$\psi = \psi_0(r) + \psi_1(r)\sin\theta$$

is a superposition of a circularly symmetric ($m = 0$) 'rider' and a dipolar ($m = 1$ circular mode) part. The latter will be assumed to have relatively small amplitude in the interior region.

2.2. *Vortices propagating with the speed of long Rossby waves*

It was demonstrated by SR that the steadily propagating solutions for the purely barotropic f-plane could be applied to the case of the equivalent barotropic β-plane model if the propagation velocity is exactly equal to the long Rossby wave (signal) velocity. This result follows from (3), which for $c = -R_d^2$ reduces to $J(\psi, \Delta\psi) = 0$. The latter equation is merely the stationary barotropic f-plane equation, for which stable and almost monopolar solutions have been obtained by SR. The dipolar component ($m = 1$) of those solutions that allow an eddy to propagate rectilinearly with the speed of the long Rossby waves was found to be

$$\left.\begin{aligned} \psi_1(r,\theta) &= -\frac{2R_d^2}{\bar{u}'(1)}\bar{u}(r)\sin\theta \quad (r < 1), \\ \psi_1(r,\theta) &= R_d^2(\tfrac{1}{r} - r)\sin\theta \quad (r > 1), \end{aligned}\right\} \tag{4}$$

where the basic azimuthal velocity $u(r) = \partial\psi_0(r)/\partial r$ is assumed to be compact (zero in the exterior $r > 1$), and $\bar{u}'(1^-) \neq 0$. The solution (4) is irrotational in the region $r > 1$ and, therefore, exactly satisfies the stationary barotropic vorticity equation in the exterior; in the interior ($r < 1$), however, the derivation of (4) assumes asymptotic smallness of the dipolar component ψ_1 compared to the basic flow ψ_0. The linear theory, therefore, additionally requires $R_d^2 \ll \max(\bar{u}(r))$, which holds for typical values of the oceanic parameters.

Thus, there exists a large class of stable quasi-monopolar vortices propagating with the speed of long Rossby waves. This analytical solution for $c = -R_d^2$ is a very important one since the numerical calculations of McWilliams & Flierl (1979), and others, suggest that an initially stationary and symmetric equivalent barotropic vortex on the beta-plane will eventually evolve towards a structure propagating westward with the velocity of the long Rossby waves.

2.3. *Vortices propagating with supercritical velocities*

Now our objective is to modify the aforementioned asymptotic solution to consider the general case $c < -R_d^2$ and $c > 0$; subcritical c are not considered here because of the intrinsic time dependence due to far-field wave radiation. As indicated previously, we look for stable solutions of (3), assuming that the streamfunction can be described as a superposition of the dominant circularly symmetric rider and a small dipolar part. Following SR, let us consider separately the region inside the unit circle streamline and the exterior flow with open streamlines surrounding the eddy. In order to avoid linearization in the far field (where the velocities are small), we use an exact solution in the exterior. The derivation of an exact solution in the region $r > 1$ (Flierl *et al.* 1980) requires a linear relationship between the arguments in the Jacobian (3): $\psi = (c/\hat{\beta})(\Delta\psi + \hat{\beta}y)$, and in terms of ψ_0, ψ_1 this reduces to

$$\psi_0'' + \frac{1}{r}\psi_0' - \frac{\hat{\beta}}{c}\psi_0 = 0 \quad (r > 1), \tag{5a}$$

and

$$\psi_1'' + \frac{1}{r}\psi_1' - \left(\frac{1}{r^2} + \frac{\hat{\beta}}{c}\right)\psi_1 + \hat{\beta}r = 0 \quad (r > 1). \tag{5b}$$

Equation (5*a*) is the well-known modified Bessel equation of zeroth order, which allows for the exponentially decaying solution,

$$\psi_0(r) = AK_0(r/\alpha) \quad (r > 1), \tag{6a}$$

where

$$\frac{1}{\alpha} = \left(\frac{\hat{\beta}}{c}\right)^{1/2}.$$

For the supercritical westward $c < -R_d^2$ or eastward $c > 0$ velocities, $\hat{\beta}/c$ is positive.

The exact solution of (5*b*) is a sum of its particular solution (cr) and the well-behaved general solution of the corresponding homogeneous equation:

$$\psi_1 = B\hat{K}_1\left(\frac{r}{\alpha}\right) + cr \quad (r > 1), \tag{6b}$$

where K_1 is the modified first order Bessel function. From the definition of α (above) we obtain the propagation velocity:

$$c = R_d^2 \frac{\alpha^2}{R_d^2 - \alpha^2}. \tag{7}$$

To obtain the solution in the interior let us linearize equation (3) in the interior region, considering ψ_1, $\hat{\beta}$, and c to be of the same order, and much smaller than ψ_0 (but no assumption has yet been made about how close the propagation velocity is to the speed of the Rossby waves). In terms of the dipolar streamfunction ψ_1, equation (3), linearized in the interior, can be written as

$$\bar{u}\left(\psi_1'' + \frac{1}{r}\psi_1'\right) - \psi_1\left(\bar{u}'' + \frac{1}{r}\bar{u}'\right) = -\hat{\beta}\bar{u}r \quad (r < 1), \tag{8}$$

where $\bar{u}$ is the undisturbed azimuthal velocity.

The boundary conditions required to match the exterior field (6*a,b*) with the solution of (8) in the interior will be those of the continuity of the azimuthal velocity, and no flow normal to the interface. The latter condition yields $\psi_1(1^-) = \psi_1(1^+) = 0$, and therefore

$$B = -\frac{c}{K_1(1/\alpha)}. \tag{9a}$$

The condition of continuity of velocity at $r = 1$ applied to the radially symmetric part of the flow determines the constant A in equation (6*a*):

$$\bar{u}(1) = \left.\frac{\partial \psi_0}{\partial r}\right|_{r=1^+} = -AK_1(1/\alpha)(1/\alpha), \tag{9b}$$

and when continuity is applied to the dipolar part of the flow, we obtain

$$\psi_1'\big|_{r=1^-} = -0.5B(K_0(1/\alpha) + K_2(1/\alpha))(1/\alpha) + U = U\left(\frac{K_0(1/\alpha)}{K_1(1/\alpha)\alpha} + 2\right). \tag{9c}$$

When $\hat{\beta}$ in (8) is eliminated using $\psi_1(r) \equiv \hat{\beta}\Phi(r)$, the result is

$$\bar{u}\left(\Phi'' + \frac{1}{r}\Phi''\right) - \Phi\left(\bar{u}'' + \frac{1}{r}\bar{u}'\right) = -\bar{u}r, \tag{10}$$

and the boundary conditions are

$$\Phi(1) = 0, \tag{11}$$

and

$$\Phi'(1) = \alpha\frac{K_0(1/\alpha)}{K_1(1/\alpha)} + 2\alpha^2. \tag{12}$$

Also, if $\bar{u}(1) \neq 0$, the boundary condition (11) applied to equation (10) yields:

$$\Phi'' + \Phi' = -1 \quad \text{at } r = 1^-. \tag{13}$$

Since it is difficult to solve (10) directly to obtain Φ for a given $\bar{u}$, a more tractable approach is to use an inverse procedure in which we assume a suitable class of dipolar streamfunctions (Φ satisfying equations (11) and (13)), and then obtain the basic velocity that allows for that disturbance. Thus, we are looking for a certain type of (form preserving) solution rather than solving a problem with specified $\bar{u}$. For this purpose, we try the following analytical function which vanishes at $r = 0$ and at $r = 1$, and satisfies (13) for all γ:

$$\Phi = -\gamma r(1 - r)\exp(-2r) + \lambda(r) \quad (r < 1), \tag{14}$$

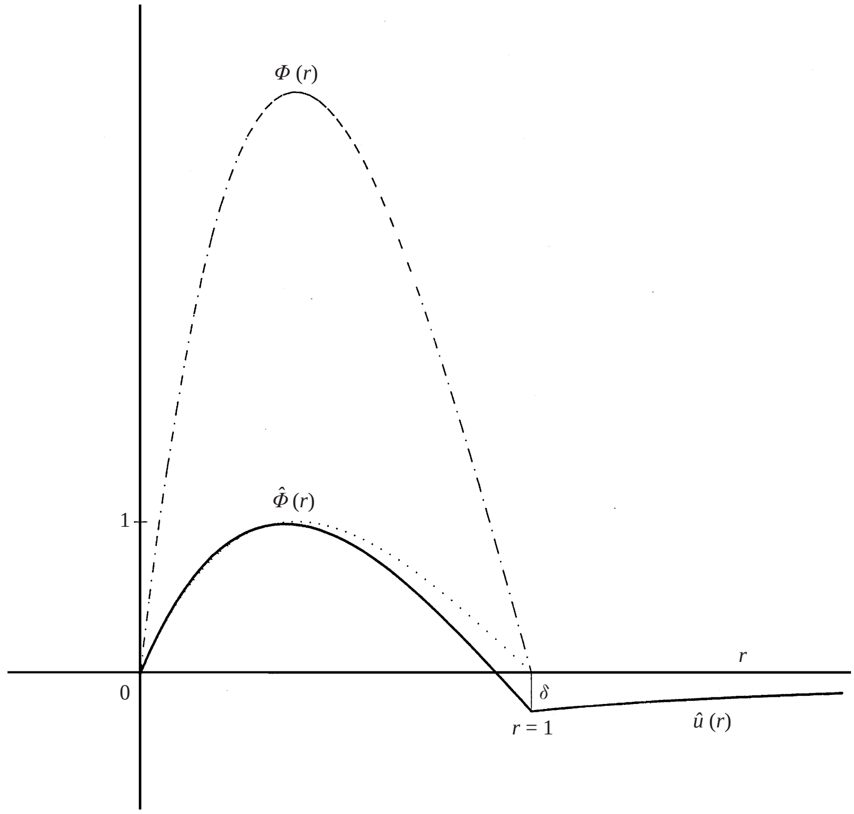

FIGURE 1. Schematic diagram of the radial components of the $m = 0$ and $m = 1$ circular modes in the interior ($r < 1$) of the vortex. $\hat{u}$ is the basic (azimuthal) velocity, normalized so that its maximum value is equal to 1. Φ is the rescaled dipolar streamfunction (see the text). The dotted curve $\hat{\Phi}$ is the dipolar streamfunction normalized so that its maximum value is equal to 1, so that it can be compared with $\hat{u}$. $\Phi, \hat{\Phi}$ and ψ_1 are exactly proportional to each other and $\bar{u}$ is almost proportional to them. For our solution (moving with a velocity comparable to the speed of the long Rossby waves) Φ is large in most of the interior ($\Phi \gg 1$). δ is the maximum difference between $\hat{u}$ and $\hat{\Phi}$, which occurs at $r = 1$ (for our particular velocity profile) and also happens to be the maximum value of the reversed (negative) velocity. Note that δ is quite small (see table 1).

where $\lambda(r) = 0.5(\gamma \exp(-2) - 1) r(1-r)^2 \exp(\gamma(r-1))$ is small for the values of parameters employed.

Now, we solve the second-order equation (10) for $\bar{u}$, using Φ as given by (14). Since equation (10) is homogeneous with respect to $\bar{u}$, all its solutions (for a fixed Φ) which satisfy condition $\bar{u}(0) = 0$ are proportional to each other, so that $\bar{u}$ may be normalized as indicated below. Equation (10) was solved numerically for different γ using a second-order Runge–Kutta scheme ($\Delta r = 0.001$) and starting with the conditions $\bar{u}(0) = 0$ and (say) $\bar{u}'(0) = 1$. This allowed us to obtain the interior basic velocity up to some constant multiplier:

$$\bar{u}(r) = u_{max}\,\hat{u}(r) \quad \text{where} \quad u_{max} = \max_{0<r<1} \bar{u}$$

and $\hat{u}$ is the basic velocity normalized so that the velocity maximum is equal to 1. The computed velocity profiles in all the experiments performed had a structure like that shown in figure 1, where the value of $\hat{u}(1)$ was a small negative number. Equation (12)

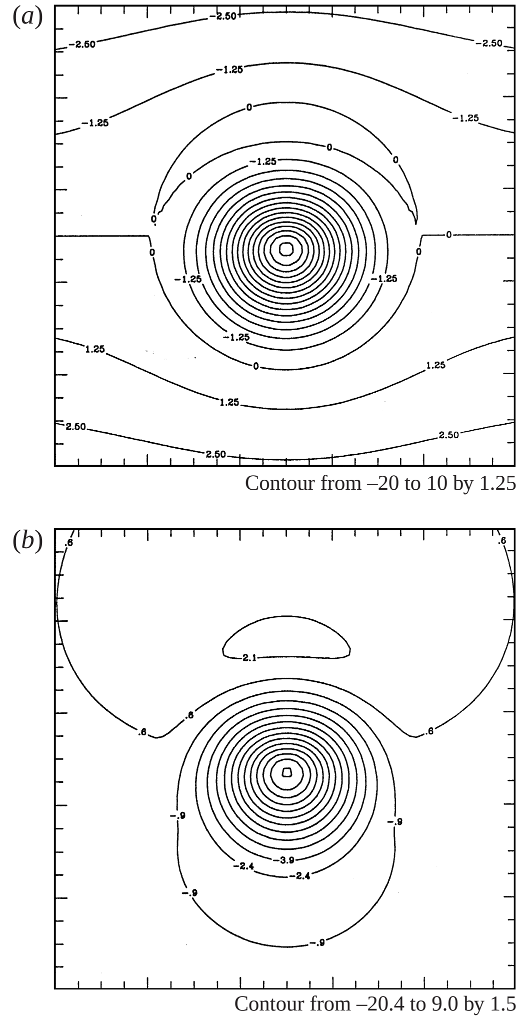

FIGURE 2. Isopleths of the streamfunction $\gamma = 36, c = -2, \bar{u}_{max} = 30$ for the analytical solution of §2. (*a*) In the frame of reference moving with the eddy. (*b*) In the stationary coordinate system.

then implicitly determined α, and the propagation velocity in units of speed of long Rossby waves was computed from (7). The $m = 0$ field in the exterior of the vortex is given by (6*a*), in which the constant A was determined from (9*b*). The exterior $m = 1$ field is provided by (6*b*). Thus, for a given γ, we determine the whole structure of the eddy and its propagation velocity.

The streamlines of the solution are presented in figure 2 for $R_d = 1$, $\gamma = 36$, which corresponds to the propagation velocity $c = -2R_d = -2$, and for $u_{max} = 30$. The structure of this vortex is quite similar to the barotropic solution of SR. Note that the value of the mean negative azimuthal velocity is relatively small in figure 2, and could probably not be detected in contemporary oceanic observations, thus such a signature of the supercritical vortices is not inconsistent with those observations.

In our work, we concentrate on large values of the parameter γ for two reasons. Large values of γ correspond to large α (see equation (12)), and large α require propagation velocities (7) to be close to the speed of the long Rossby waves. These velocities are the most interesting ones, since the oceanic vortices are known to propagate with comparable speeds. Also note that equation (10) is homogeneous with respect to $\bar{u}$, but not homogeneous with respect to Φ. So for large $\Phi \gg 1$, equation (10) might be approximated by $\bar{u}(\Phi'' + (1/r)\Phi') - \Phi(\bar{u}'' + (1/r)\bar{u}') = 0$ which allows for only one well-behaved solution in which the dipolar streamfunction is proportional to the velocity:

$$\bar{u}(r) = C\Phi(r) \quad (r < 1). \tag{15}$$

This important feature of the propagating vortices is referred to as an 'alpha gyre' (see SR). Also note that the particular Φ employed (equation (14)) has an extremum not too far from $r = 0$ (see figure 1), and equation (15) suggests the maximum of the azimuthal velocity $\bar{u}$ will also occur sufficiently close to $r = 0$. So, the vortex is expected to be stable, as inferred from the result of Flierl (1988). Figure 1 reveals how, for large γ, the functions Φ and $\bar{u}$ can be approximately proportional to each other, even though $\bar{u}$ changes sign in the interval $0 < r < 1$. Also note that large values of Φ (figure 1) do not mean large values of $\psi_1 = \hat{\beta}\Phi$, since as $\gamma \to \infty$ (and $\Phi \to \infty$) $\hat{\beta} \to 0$, and the dipolar moment ψ_1 remains finite and much smaller than ψ_0.

2.4. *Significance of alpha-gyres*

In the previous subsection we have shown that, in the limit $c \to -R_d^2$ (corresponding to $\gamma \to +\infty$), the dipolar component of the streamfunction Φ is proportional to the basic velocity $\bar{u}$. Let us see now how close the relationship between the $m = 0$ and $m = 1$ modes is to the alpha-gyre relationship for other values of the propagation velocity. Unfortunately, we cannot simply divide $\bar{u}$ by Φ and check whether the ratio is a constant because Φ is zero at $r = 0, 1$; instead we introduce another measure indicative of the extent to which $\bar{u}$ and Φ are proportional to each other. Let us normalize both $\bar{u}$ and Φ so that their maximum value will be equal to 1:

$$\hat{u} = \frac{\bar{u}}{u_{max}}, \quad \hat{\Phi} = -\frac{\Phi}{\Phi_{max}},$$

where

$$u_{max} = \max_{0<r<1} \bar{u}, \quad \Phi_{max} = \max_{0<r<1}(-\Phi).$$

($\hat{\Phi}$ is presented in figure 1 by a dotted line). Then the difference

$$\delta = \max_{0<r<1} |\hat{u} - \hat{\Phi}|$$

will show how close our solution is to the alpha-gyre. Note that for the $c = -R_d^2$ case, $\hat{u} = \hat{\Phi}$ and, therefore, δ is exactly zero. The maximum difference between $\hat{u}(r)$ and $\hat{\Phi}(r)$ happens to occur at $r = 1$, therefore δ is also equal to the maximum value of the negative basic (normalized) velocity. Table 1 shows how δ depends on the propagation velocity (i.e. on the value of the parameter γ). We see that the dipolar part of the streamfunction is nearly an alpha-gyre for a wide range of propagation velocities, which include all the westward propagating eddies, and even the fast eastward propagating solutions. The alpha-gyre relationship (15) means that the interior undisturbed circular streamlines and vorticity isopleths (except those near $r = 1$) are displaced in the y-direction by the same amount (see SR).

Another important feature of the $1\frac{1}{2}$-layer solution is that it has a vanishing angular

γ	c	$\delta = \max\lvert\hat{\Phi} - \hat{u}\rvert$	α
100	−1.19	0.0098	2.47
50	−1.53	0.017	1.70
30	−2.62	0.028	1.27
15	2.42	0.055	0.84
10	0.74	0.08	0.65

TABLE 1. The small values of δ show that the radial component of the streamfunction is similar to the alpha-gyre. Comparison is made by normalizing both $\bar{u}$ and Φ and computing the maximum difference δ. The limit $\gamma \to +\infty$ corresponds to the vortices propagating exactly with the signal velocity of the long Rossby waves, in which case the streamfunction Φ is exactly proportional to the basic velocity.

momentum, or (if $\hat{\beta} \neq 0$)

$$\int_{2\pi}\int_0^{+\infty} \psi(r,\theta) r\,\mathrm{d}r\,\mathrm{d}\theta = \int_{-\infty}^{+\infty}\int_{-\infty}^{+\infty} \psi\,\mathrm{d}x\,\mathrm{d}y = 0. \tag{16}$$

This is proved by multiplying (10) with r and integrating (in the interval $0 < r < 1$) by parts to obtain

$$\int_0^1 \bar{u}(r)\,r^2\,\mathrm{d}r = -\Phi'(1)\,\bar{u}(1). \tag{17}$$

When equation (6*a*) is used to compute $\int_1^{+\infty} \bar{u}(r)\,r^2\,\mathrm{d}r$, and when the result is simplified using the basic relationships between the Bessel functions (Abramowitz & Stegun 1979) and equation (12), we obtain:

$$\int_1^{+\infty} \bar{u}(r)\,r^2\,\mathrm{d}r = \frac{\bar{u}(1)}{K_1(1/\alpha)}\int_1^{+\infty} K_1\left(\frac{r}{\alpha}\right) r^2\,\mathrm{d}r = \Phi'(1)\,\bar{u}(1).$$

Adding the last two results gives zero angular momentum, or (16).

Because of (16) our solution does not contradict the (aforementioned) centroid theorem (McWilliams & Flierl 1979) which states that the centroid of any sufficiently compact smooth structure should move exactly with the speed of the long Rossby waves if its angular momentum is non-zero (the term 'centroid' here refers to the interfacial density displacement).† (This theorem was subsequently rederived by Cushman-Roisin, Chassignet & Tang 1990 and by Nycander & Sutyrin 1992.) It is a commonly accepted notion that all the possible steadily propagating solutions satisfying (16) are either dipolar vortices (such as the modons), or strongly unstable structures (e.g. modon-with-a-rider solution of Flierl *et al.* 1980). This notion is without basis, as our solution clearly demonstrates.

3. Numerical calculations

In the previous section we presented a class of quasi-monopolar eddies that are able to propagate with arbitrary supercritical velocities. Now we examine numerically the

† The requirement of zero angular momentum also appears in another fundamental geophysical theorem derived by Flierl, Stern & Whitehead (1983) who demonstrated that the barotropic component of isolated beta-plane vortices cannot be monopolar, which was quantified by requirement (16). The latter result, however, is not directly applicable to the case of a model with an infinitely deep lower layer. The monopolar rotation in the thin upper layer can be compensated by a weak motion in the lower layer. The limit of an infinite lower-layer depth corresponds to the absence of motion there, creating a false impression of monopolar barotropic circulation in the model.

stability of the eddy (since the conventional analytical normal mode analysis of such a problem appears to be intractable), and determine the extent to which our linear steady-state solution is realizable in the sense of an initial-value calculation. This work extends that of McWilliams & Flierl (1979), Mied & Lindemann (1979), and others which suggest that a monopolar quasi-geostrophic eddy on a β-plane evolves to a structure propagating with the speed of long Rossby waves. The long-time evolution of an eddy is especially interesting in our case since the angular momentum (16) is zero and, therefore, the eddy is free from the restriction on the propagation velocity posed by the centroid theorem.

3.1. *Numerical experiments initiated by the steady-state solution*

The numerical calculations have been performed using a pseudo-spectral code (Canuto *et al.* 1987) in which the spatial operators were exactly inverted in Fourier space. The quasi-geostrophic potential vorticity equation (1) has been discretized on a 128×128 biperiodic grid with grid spacing $\Delta x = \Delta y = 0.05$. A fourth-order Runge–Kutta scheme with timestep $\Delta t = 0.003$ was used for integration in time. Numerical stability of the code was controlled by the dissipational functional $\nu \Delta^n \psi$, with $n = 4$ and $\nu = 5 \times 10^{-8}$, added to the right-hand side of (1). The experiments were initiated by the linear solution presented in the previous section and the calculations were confined to the case where the radius of deformation is the same as the radius of the eddy. In the following experiments we normalized the symmetric part of the solution by taking the successive values of velocity maximum to be 10, 20, 30 or 40 units; this range describes mid-ocean vortices having a maximum radial velocity of about 50–120 cm s^{-1} and propagating with a speed of 2–5 cm s^{-1}.

As we can see from figure 3 the vortex, whose $\bar{u}_{max} = 30$ and $c = -2R_d^2 = -2$ initially, is moving almost exactly in the westward direction (similar behaviour was seen in most of the experiments made with westward propagating vortices), and only after a sufficiently large period of time was a northward component of propagation velocity observed. This feature distinguishes our experiments from those initiated by the completely symmetric vortices (e.g. McWilliams & Flierl 1979; Mied & Lindemann 1979) in which the initial motion was northward (southward for the anticyclones).

The x-coordinate of the potential vorticity maximum for the calculation in figure 3 is given by the thick line curve in figure 4; the thin solid line corresponds to propagation with the theoretical velocity (see § 2). Although theoretical and observed velocities agree initially, the latter eventually reduces to the speed of the long Rossby waves (dashed line in figure 4). A similar decay has been observed in all experiments with westward propagating vortices; in some cases the eddies slowed down to a speed of less than $-R_d^2$, but the difference was small enough to be attributed to numerical effects, such as artificial periodicity. Thus, the foregoing calculations indicate that motion with the speed of the long Rossby waves is in fact a preferred state for strong vortices. The eddy fails to maintain the supercritical velocity predicted by the linear theory because the latter is not uniformly valid in time (see Stern & Radko 1998 for an estimate of the period of validity of a similar steady-state eddy model).

3.2. *Timescale of adjustment to the propagation with the speed of the long Rossby waves*

Define t^* as the time when the actual propagation velocity (c^*) drops to the average of the initial ($c < 0$) velocity and the Rossby wave velocity $-R_d^2$:

$$c^* = 0.5(c - R_d^2).$$

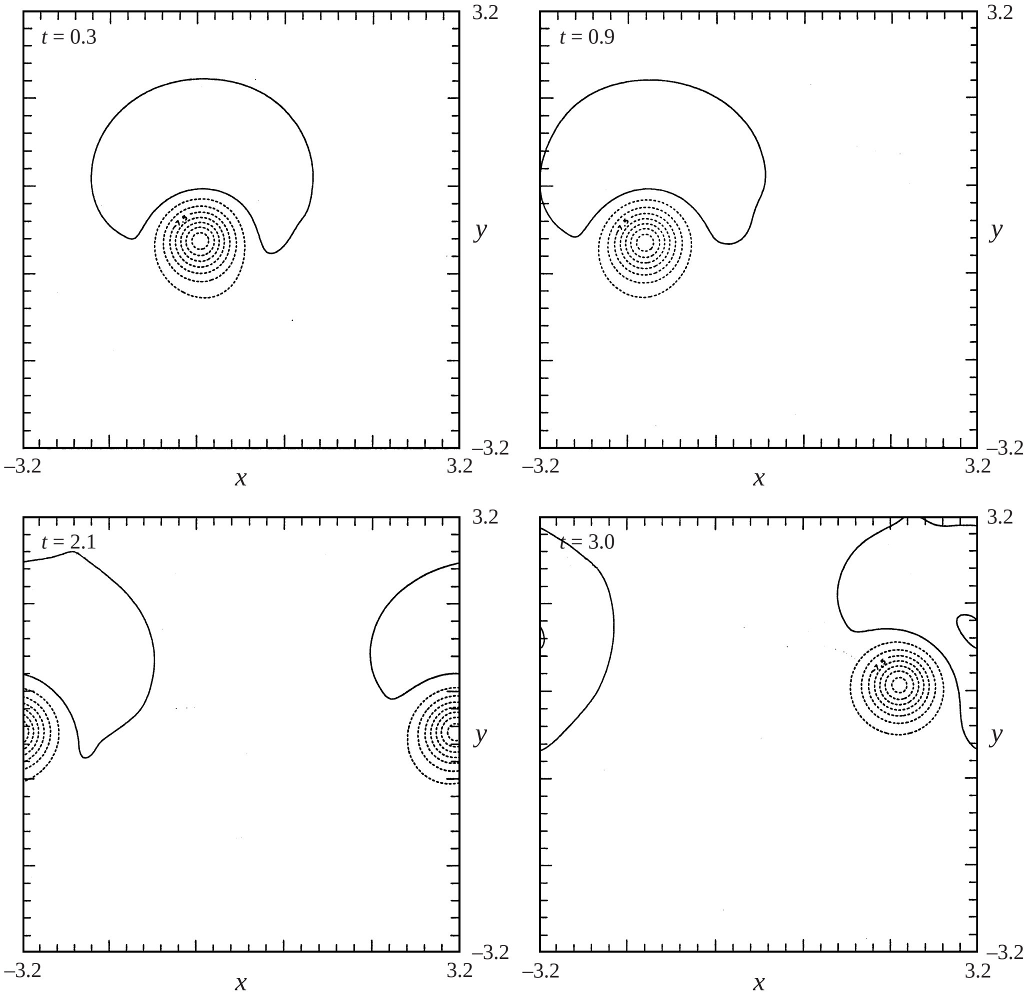

FIGURE 3. Numerical solution of the equivalent-barotropic vorticity equation. Streamlines of the westward propagating vortex at $t = 0.3, 0.9, 2.1$ and 3.0. The contour interval is 2.5. Positive contours are solid lines. The initial propagation velocity is twice the speed of the long Rossby waves. The maximum azimuthal velocity (initially) is 30 in units of the speed of the Rossby waves. Note that initially the eddy is preserving its shape (compare with figure 2 *b*).

This quantity t^* can be thought of as a period of time when the eddy retains the memory of its initial conditions. We performed a series of experiments with different values of the strength of the basic symmetric azimuthal current and the (initial) propagation velocity. The results (table 2) show that for westward eddies, t^* increases with $\bar{u}$ and then levels off or decreases. Maximum t^* occurs at high $\bar{u}$ when the propagation velocity is small, but is shifted to relatively low $\bar{u}$ when the velocity is large. We believe that these calculations (t^*) adequately represent the timescale involved in the adjustment of a β-plane vortex towards the final state, but the initialization based on our analytical (linear) theory may introduce a biased effect. From table 2 we find that our vortex is able to preserve its initial speed throughout 30 revolutions of the particles (with maximum velocity) around the centre, and during

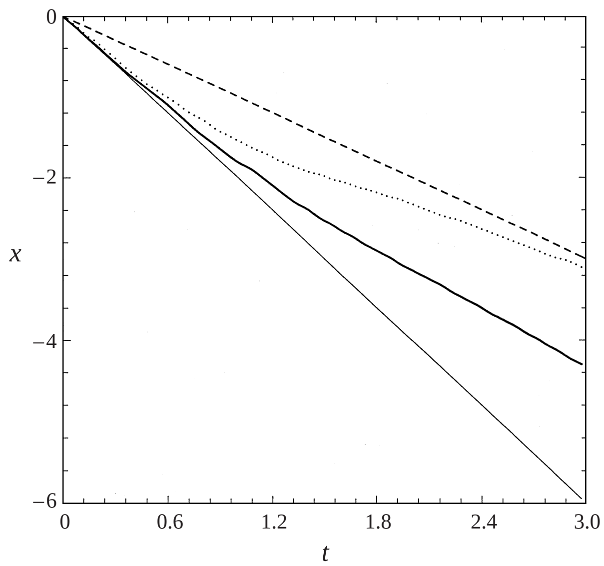

FIGURE 4. ——, x-coordinate of the centre of the vortex as a function of time for zero angular momentum initialization; ——, coordinate of a point moving with the theoretical velocity; – – – –, coordinate of a point moving with the velocity of the long Rossby waves; · · ·, experiment made with the 'pure alpha-gyre' solution (see equation (18)). In both experiments the vortex is initially moving with the predicted theoretical velocity; later on, the vortex slows down to the speed of the long Rossby waves. The numerical experiments were made for westward propagating vortices, moving initially with a propagation velocity twice the speed of the long Rossby waves and a maximum azimuthal velocity 30 times as great (see also figure 3).

c	$u_{max} = 10$	$u_{max} = 20$	$u_{max} = 30$	$u_{max} = 40$
1.5	5	14	14	15
2.0	5	18	14	14
2.5	5	20	13	9
−1.0	>8	7.1	> 8	3.1
−2.0	>8	> 8	3.1	3.8

TABLE 2. The upper part of the table, for westward vortices, gives the value of t^* as a function of non-dimensional vortex strength u_{max} and initial propagation velocity c. The lower part of the table (last two rows), for vortices initially moving eastward, gives the total propagation distance (see text) as a multiple of the eddy radius.

this time the vortex can travel a distance of up to 4 radii. The eddy will, of course, continue propagating westward much further than this, but with a lower speed.

Unlike the westward vortices the eastward eddies cease propagating (to the east) after going a finite distance (table 2). For these vortices the natural criterion of their ability to remember the initial conditions is the maximum eastward displacement. In eight experiments made with eastward vortices, the propagation distance was more than 8 radii in four runs. Unlike the westward propagating cyclonic vortices, the eastward ones (not shown) exhibit significant deflection to the north. This displacement results in the decrease of the cyclonic rotation, while the amplitude of the small anticyclonic companion increases, as required by the conservation of potential vorticity.

3.3. *Effect of the non-zero angular momentum*

As indicated, the eddy used to initiate the previous spectral calculations had zero angular momentum (as required by the centroid theorem (McWilliams & Flierl 1979) for steady supercritical propagation). The possibility of different dynamics for eddies with finite angular momentum is now considered by using an eddy whose dipolar component (and therefore propagation velocity) is exactly the same as given in § 2 (see equations (6*b*) and (14)), but whose basic azimuthal velocity is changed so that it is positive everywhere in the interior ($r < 1$) and zero in the exterior ($r > 1$). The technically simplest way to make such a change is to assume a 'pure' alpha-gyre relationship between $m = 0$ and $m = 1$ modes:

$$\begin{cases} \bar{u}(r) = C\Phi(r) & (r < 1), \\ \bar{u}(r) = 0 & (r > 1), \end{cases} \tag{18}$$

where Φ is still given by (14) and C is an arbitrary (sufficiently large) number. As table 1 shows (see also figures 1 and 2) this alteration only makes a small change in the $m = 0$ mode, but the new eddy (18) does not satisfy condition (16) of the centroid theorem.

Using the previous spectral code we computed the evolution of this new initial state whose strength and the propagation velocity were the same as for the vortex in figure 3. The centre of the eddy, defined by the point of maximum potential vorticity and shown by the dotted line in figure 4, moves for a significant time with the velocity given by the previous analytic theory, but later it slows down to a speed which is slightly less than that of the long Rossby waves. The period of time needed for such a change in propagation velocity is about 1 time unit, which is less than the adjustment time for a zero angular momentum eddy (solid line in figure 4). During this time, however, the eddy can propagate a distance of about one diameter and the particles in the interior are able to perform up to 15 revolutions around the centre. This example shows how the 'local' (and more physically significant) centre of the eddy can move with a speed different from that required by the 'global' interfacial centroid theorem.

The robustness of these conclusions from the $1\frac{1}{2}$-layer model has been examined by extending the numerical experiments to a two-layer model. The results for runs made with 1 : 4 and 1 : 8 upper/lower layer depth ratios were in qualitative agreement with the present equivalent barotropic calculations, when the initial conditions were similar. Radko (1997) gives details of the two-layer calculations.

4. Development of the dipolar component on the beta-plane vortices

In our numerical calculations, as well as in the other cited experiments, the eddy propagation speed evolves to that of the long Rossby waves. Since it was shown (§ 2) that the critical and slightly supercritical eddies may be of the specific 'alpha-gyre' type, the question arises as to the extent to which the final state contains the alpha-gyre component. To answer this we will Fourier analyse numerical solutions for the evolution of an initially symmetric vortex on the β-plane.

The main difficulty here, however, is that when we decompose the streamfunction field into the circular Fourier components, it is difficult to accurately determine the relevant $m = 1$ circular mode, since its amplitude is very sensitive to the chosen position of the polar centre. Additional complications arise if (as occurs in our analytical solution) the interior structure of the vortex is almost uniformly shifted relative to its boundary ($r = 1$). Then the only way to determine such a shift is to first calculate the coordinates of the centre from the vortex exterior and then relate to the inner structure of the eddy. Most methods for determining the centre of an eddy (such as the alpha-gyre closure method in Willoughby (1992), or the centre of mass estimate in Hooker & Olson (1984)) are based on the information from the area which includes the eddy interior. Since now it is necessary to introduce a procedure that estimates the position of the polar centre of an eddy in a way which does not depend on the details of the interior field, we shall pivot the analysis about the bounding streamline of the eddy.

We first consider the evolution of an initially symmetric compact equivalent barotropic vortex on the β-plane (following the initial-value calculations of McWilliams & Flierl (1979) for a Gaussian vortex). The integration in time of the equivalent-barotropic vorticity equation (1) was performed using the pseudo-spectral code described and used in § 3, and initialized by the azimuthal velocity field:

$$u(r) = ar(1-r)\,\mathrm{e}^{-2r} \quad (r < 1),$$
$$u(r) = 0 \quad (r > 1).$$

The value of a was chosen to give a maximal azimuthal velocity equal to 20, which adequately represents an average oceanic eddy. The radial velocity was zero initially and the radius of deformation (again) was $R_d = 1$.

As expected, this vortex starts to move northward, then gradually turns to the west, and by time $t = 17.5$ its motion is almost exactly westward. The vortex motion is accompanied by a radiation of Rossby waves in a wake behind the vortex, and this radiation reduces the strength of the vortex by 10 % at $t = 7.5$. At this time the vortex approaches the velocity of the longest Rossby waves (based on the finite x-boundaries in our computational domain), and subsequently the maximum azimuthal velocity changes very slowly in the later stage of the experiment. The scenario of the evolution of a compact vortex described above agrees qualitatively with the results obtained by McWilliams & Flierl (1979) for the Gaussian vortex.

The large azimuthal velocities of this strong eddy result in the formation of two distinct regions: a region of trapped fluid in the interior of the vortex characterized by closed streamlines (in the moving coordinate system), and an outer region with open streamlines. Let us define the centre of an eddy as the centroid of an area bounded by the largest closed streamline in a frame of reference moving with an eddy. This definition is consistent with the one we used in § 2, when the condition of no flow normal to the interface $r = 1$ was prescribed. A method (Radko 1997) which allows us to efficiently estimate the coordinates of such a streamline assumes that the largest closed streamline is almost circular (owing to the well-known (Sutyrin 1989) symmetrization property of intense vortices), which will be confirmed in our numerical experiments. The actual numerical procedure involves a 'shooting method', in which we consider a large number of trial centres (x_0, y_0) in the interior of the eddy and check which one is a centre of the largest closed circular streamline.

This technique was applied to the streamfunction field at $t = 7.5, 12.5$ and 17.5 to obtain the coordinates of the centre of the vortex, and figure 5 presents the streamlines in the stationary system at $t = 17.5$. The square denotes the point of maximum relative vorticity, and the small circle marks the centre of the vortex computed by our method. We can see that the inner streamlines are shifted southward with respect to our computed centre. The streamfunction in the moving system (not shown), obtained from $\psi_{stationary} = \psi_{moving} - cy$, clearly demonstrates that the interior streamlines are

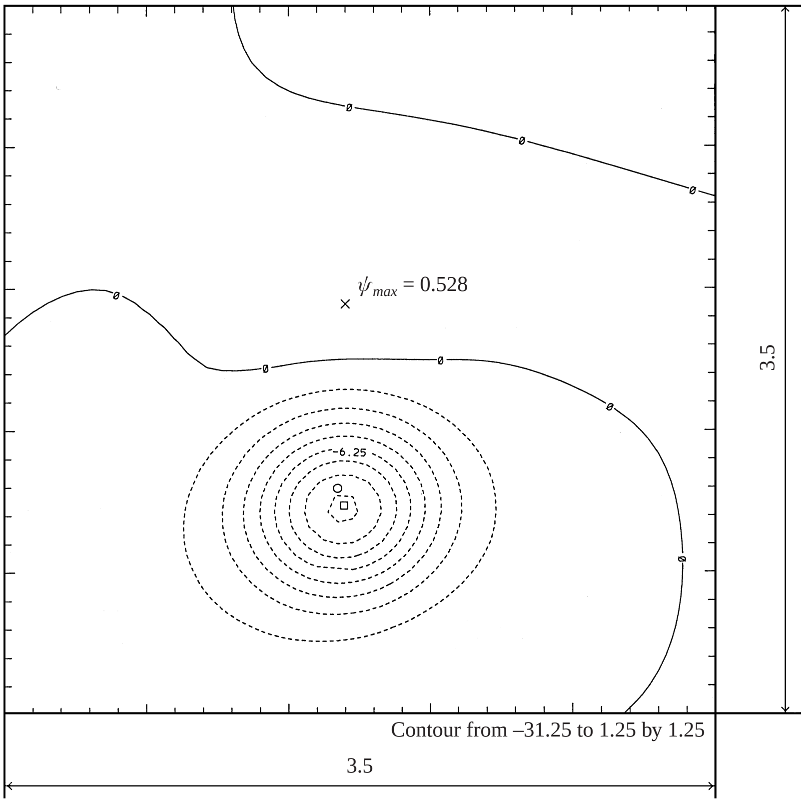

FIGURE 5. The streamlines in a stationary coordinate system of the vortex which evolved to an almost steady propagating structure at $t = 17.5$ from a circularly symmetric initial state. The square denotes the point of the maximum vorticity and the circle denotes the centre of the eddy computed using the technique described in § 4. The scale of the plot (in both x and y) is 3.5 times the vortex radius. Note the pressure maximum leading to a current reversal of small magnitude.

almost circular, but they are shifted southward compared to the position of the largest closed streamline; this is a characteristic feature of an alpha-gyre.

After the coordinates of the 'correct' centre of the eddy were obtained, the streamfunction field was interpolated to the polar coordinates grid using the collocation approximation with the centre of the polar coordinate system placed at the centre of the vortex. The polar coordinates grid had $\Delta r = 0.025$, $\Delta\theta = 2\pi/32$. For each r the streamfunction was Fourier analysed in θ, using the fast Fourier transform. Of particular interest for our problem are the $m = 0$ and $m = 1$ Fourier components. Figures 6(a), 6(c) and 6(e) show the radial part of the $\sin\theta$ component of the streamfunction; and figures 6(b), 6(d) and 6(f) show the first derivative of the $m = 0$ mode, which is the basic azimuthal velocity, at times $t = 7.5, 12.5$ and 17.5, respectively. From figure 6 we can clearly see that the radial component of the dipolar streamfunction is proportional to the basic velocity. Thus, the propagating solution resulting from the evolution of the symmetric vortex on the beta-plane obeys our linear theory: the dipolar part of the streamfunction is indeed an alpha-gyre. This particular result is not very sensitive to the accuracy with which we determined the coordinates of the centre of the vortex. If there is a certain error in the coordinates of the centre, it would result in the appearance of an additional component of the dipolar part of the streamfunction which is again spatially distributed in the form of an alpha-gyre.

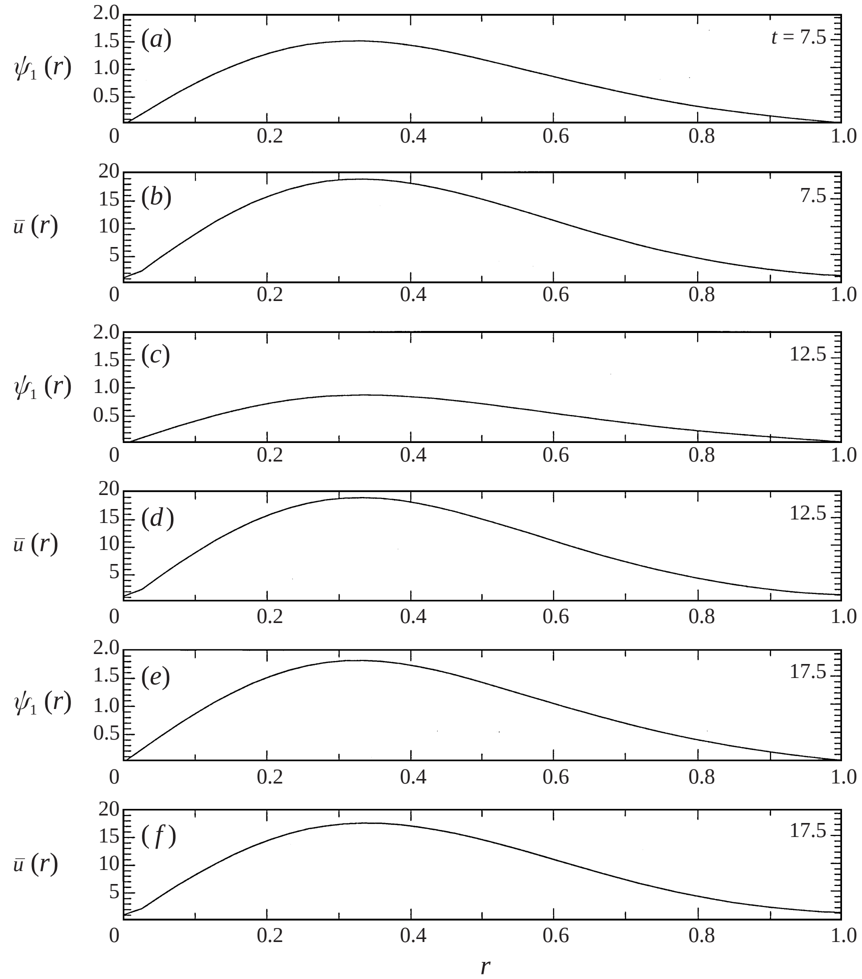

FIGURE 6. Circular Fourier analysis of the streamfunction field of the westward propagating vortex which evolves from the initially symmetric eddy on the beta-plane. (*a*) Radial part $\psi_1(r)$ of the dipolar component ($m = 1$ mode) of the streamfunction as a function of r. The non-dimensional value of time $t = 7.5$. (*b*) Circularly symmetric part of the velocity field $\bar{u}(r)$ ($m = 0$ mode). The dipolar streamfunction is proportional to the azimuthal velocity, in agreement with the predicted alpha-gyre relationship. (*c*) The same as (*a*), but for $t = 12.5$. (*d*) The same as (*b*), but for $t = 12.5$. (*e*) The same as (*a*), but for $t = 17.5$. (*f*) The same as (*b*), but for $t = 17.5$.

So the 'correct' $m = 1$ mode would be a difference between the two dipolar components both of the alpha-gyre type and therefore it would also be an alpha-gyre. The connection between rectilinear propagation and the alpha-gyre structure of an eddy was suggested by our analytical theory for the supercritical eddies, and now we have demonstrated numerically such a relation for the 'naturally evolved' slightly subcritical eddy.

In our previous work (SR), a simple formula suggested as an estimate of the propagation velocity of barotropic f-plane compact eddy is:

$$\psi_1'(1) = -2c, \tag{19}$$

where $\psi_1(r)$ denotes the radial part of the $m = 1$ mode. Furthermore, it was shown in

§ 2 that this solution is immediately applicable to the equivalent barotropic β-plane model if the propagation velocity is sufficiently close to the speed of the long Rossby waves. For our 'naturally evolved' steady westward propagating eddy the error in the propagation velocity computed from (19) compared to that measured experimentally is 10 %, 26 % and 16 % for $t = 7.5, 12.5$ and 17.5, respectively. Therefore, (19) gives a reasonably good estimate of the propagation velocity of the eddies, which provides an indirect check of the numerical method employed above, and might also be applied to the observations of oceanic eddies.

5. Conclusions and discussion

A perturbation theory for a nearly symmetric eddy on the β-plane shows that it is able to propagate either westward, with a uniform speed exceeding that of long planetary waves, or eastward. The alpha-gyre structure of the vortex is similar to that of the propagating barotropic f-plane solution (SR), and can be characterized by a uniform shift of the interior of the eddy in a direction perpendicular to the direction of propagation. The numerical calculations in § 3 demonstrate the stability and robustness of the solution, distinguishing it from the vortex consisting of a modon with a rider (Flierl *et al.* 1980).

The numerical (spectral) simulations initiated with our analytical solution for the supercritical vortices showed that the velocity of a westward propagating eddy decreases slowly to a value equal to the phase speed of the long Rossby waves. These analytical and experimental results complement previous numerical simulations using initially symmetric vortices, which also evolved so as to propagate with the speed of the planetary waves. The time (table 2) involved in the process of adjusting to the final propagation speed depends on the strength of the vortex and on its initial propagation velocity. Our vortex was able to retain its initial dipole moment throughout 30 particle revolutions around the centre, while traversing a distance of about four radii. Calculations in a realistic oceanic range of parameters showed that the memory of initial conditions is longest for strong vortices when the initial propagation velocities are close to the speed of the long Rossby waves, and for vortices of moderate strength when the initial velocities are large. Of course, the eddy continues propagating westward after reaching the long wave speed.

In connection with the ability of the vortices to propagate for significant times with supercritical speeds, we remark that some of the supercritical eddies frequently observed in the ocean move up to five times faster than the long Rossby waves (Gordon & Haxby 1990; Olson & Evans 1986). Our results suggest that this might reflect a stage when the eddies are moving with arbitrary velocities proportional to an initial dipole ($m = 1$) mode, which may be generated by the mechanisms different from the β-effect, such as interactions of those eddies with topography, boundaries or currents (SR).

A supercritical eddy was observed in the South Atlantic ocean in 1989 (Duncombe Rae *et al.* 1992). To the north of a dominant anticyclonic vortex was attached a small cyclonic companion, and the whole structure was quite similar to what we have suggested as a model of a propagating eddy (figures 2, 3). The observed propagation velocity during April and May was $6.4\,\mathrm{cm\,s^{-1}}$, while the theoretical speed of the westward translation estimated by Cushman-Roisin *et al.* (1990) was only $2\,\mathrm{cm\,s^{-1}}$. In May–June, however, the observed ring did slow down to a speed of $2.1\,\mathrm{cm\,s^{-1}}$, and this evolution agrees qualitatively with the scenario suggested by our simple equivalent-barotropic model.

In § 4 we demonstrated the development of an alpha-gyre in the evolution of an originally symmetric vortex, and this result emphasizes the significance of our propagating solutions presented in § 2. Our alpha-gyre eddies should no longer be treated only as one possible form of the propagating vortices, these solutions could be expected to appear in the evolution of any sufficiently strong and compact circular vortex on the β-plane.

In the process of showing that symmetric eddies develop an $m = 1$ mode proportional to the basic velocity in the interior we developed a new method of determining the centre of an eddy. This method allows a polar Fourier analysis to be meaningfully performed, whereby the relative displacement of the interior field of an eddy can be obtained.

REFERENCES

Abramowitz, M. & Stegan, I. A. 1979 *Handbook of Mathematical Functions* (in Russian). Nauka, Moscow. 832 pp.

Canuto, C., Hussaini, M. Y., Quarteroni, A. & Zang, T. A. 1987 *Spectral Methods in Fluid Dynamics*. Springer. 567 pp.

Chassignet, E. P., Olson, D. B. & Boudra, D. B. 1990 Motion and evolution of oceanic rings in a numerical model and in observations. *J. Geophys. Res.* **95**, 22 121–22 140.

Cushman-Roisin, B., Chassignet, E. P. & Tang, B. 1990 Westward motion of mesoscale eddies. *J. Phys. Oceanogr.* **20**, 758–768.

Duncombe Rae, C. M., Shillington, F. A., Agenbag, J. J., Taunton-Clark, J. & Grundlingh, M. L. 1992 An Agulhas ring in the South Atlantic Ocean and its interaction with the Benguela upwelling frontal system. *Deep-Sea Res.* **39**, 2009–2027.

Flierl, G. R. 1988 On the instability of geostrophic vortices. *J. Fluid Mech.* **197**, 349–388.

Flierl, G. R., Larichev, V. D., McWilliams, J. C. & Reznik, G. M. 1980 The dynamics of baroclinic and barotropic solitary eddies. *Dyn. Atmos. Oceans* **5**, 1–41.

Flierl, G. R., Stern, M. E. & Whitehead Jr, J. A. 1983 The physical significance of modons: laboratory experiments and general integral constraints. *Dyn. Atmos. Oceans* **7**, 233–263.

Gordon, A. L. & Haxby, W. F. 1990 Agulhas eddies invade the South Atlantic: Evidence from geostat altimeter and shipboard conductivity-temperature-depth survey. *J. Geophys. Res.* **95**, 3117–3125.

Hooker, S.B., Brown, J. W., Kirwan Jr, A. D., Lindemann, G. L. & Mied, R. P. 1995 Kinematics of a warm-core dipole ring. *J. Geophys. Res.* **100**, 24 797–24 809.

Hooker, S. B. & Olson, D. B. 1984 Center of mass estimation in closed vortices: A verification in principle and practice. *J. Atmos. Ocean Tech.* **1**, 247–255.

Kamenkovich, V. M., Koshlyakov, M. N. & Monin, M. N. 1986 *Synoptic Eddies in the Ocean.* Reidel, Netherland. 475 pp.

Killworth, P. D. 1986 On the propagation of isolated multilayer and continuously stratified eddies. *J. Phys. Oceanogr.* **16**, 709–716.

Larichev, V. D. & Reznik, G. M. 1976 Two-dimensional solitary Rossby waves. *Dokl. Akad. Nauk SSSR* **231**, 1077–1079.

McWilliams, J. C. & Flierl, G. R. 1979 On the evolution of isolated, nonlinear vortices. *J. Phys. Oceanogr.* **9**, 1155–1182.

Mied, R. & Lindemann, G. J. 1979 The propagation and evolution of cyclonic Gulf Stream rings. *J. Phys. Oceanogr.* **9**, 1183–1206.

Mied, R. P., Lindemann, G. J. & Bergin, J. M. 1983 Azimuthal structure of a cyclonic Gulf Stream ring. *J. Geophys. Res.* **88**, 2530–2546.

Nycander, J. & Sutyrin, G. G. 1992 Steadily translating anticyclones on the beta-plane. *Dyn. Atmos. Oceans* **16**, 473–498.

Olson, D. B. 1980 The physical oceanography of two rings observed by the cyclonic ring experiment. Part II: Dynamics. *J. Phys. Oceanogr.* **10**, 514–528.

Olson, D. B. & Evans, R. H. 1986 Rings of the Aghulhas current. *Deep-Sea Res.* **33**, 27–42.

Radko, T. 1997 Theoretical studies in mesoscale jets and vortices. PhD thesis, Florida State University, Tallahassee. 129 pp.

Stern, M. E. 1975 Minimal properties of planetary eddies. *J. Mar. Res.* **33**, 1–13.

Stern, M. E. 1987 Horizontal entrainment and detrainment in large-scale eddies. *J. Phys. Oceanogr.* **17**, 1688–1695.

Stern, M. E. & Radko, T. 1998 The self propagating quasi-monopolar vortex. *J. Phys. Oceanogr.* **28**, 22–39.

Sutyrin, G. G. 1987 The beta-effect and the evolution of a localized vortex. *Sov. Phys. Dokl.* **32**, 791–793.

Sutyrin, G. G. 1989 Azimuthal waves and symmetrization of an intense vortex. *Dokl. Akad. Nauk SSSR* **304**, 1086–1091.

Sutyrin, G. G. & Flierl, G. R. 1994 Intense vortex motion on the beta plane: development of the beta gyres. *J. Atmos. Sci.* **51**, 773–790.

Swenson, M. 1987 Instability of equivalent-barotropic riders. *J. Phys. Oceanogr.* **17**, 492–506.

Willoughby, H. E. 1992 Linear motion of a shallow-water barotropic vortex as an initial-value problem. *J. Atmos. Sci.* **49**, 2015–2031.